

**SIMULATION OF GENERATION, PROPAGATION AND
RUNUP DUE TO THE 26 DECEMBER 2004
ANDAMAN TSUNAMI**

KEW LEE MING

UNIVERSITI SAINS MALAYSIA

2009

**SIMULATION OF GENERATION, PROPAGATION AND
RUNUP DUE TO THE 26 DECEMBER 2004
ANDAMAN TSUNAMI**

by

KEW LEE MING

**Thesis submitted in fulfillment of the requirements
for the degree of
Master of Science**

February 2009

ACKNOWLEDGEMENTS

I would like to record my deepest appreciation to my supervisor, Associate Professor Ahmad Izani Md. Ismail for his constant encouragement and guidance towards assisting me in achieving the objectives for this thesis. Further, I am greatly indebted to my co-supervisor Professor Koh Hock Lye for his stimulating suggestions and dedications that lead to the completion of this thesis. Also, I would like to extend my sincere appreciation to Dr. Teh Su Yean for her advice and recommendation to accomplish the thesis.

Further, I would like to take this opportunity to acknowledge USM fellowship for the financial support throughout the studies. In addition, I am grateful to the Institute for Mathematical Sciences, National University of Singapore, who had provided me a financial support to participate in a workshop in January 2008. Moreover, the School of Mathematical Sciences and the Institute of Post Graduates Studies have provided me various facilities and information for me to conduct this research, which I would like to acknowledge. Last but not least, I would like to thank my family for their unconditional support during time of stress and duress. Finally, I would also like to take this opportunity to record my appreciation to my friends, who have provided me joys and wonderful fond memory during my graduate study.

TABLE OF CONTENTS

	Page
ACKNOWLEDGEMENTS	ii
TABLE OF CONTENTS	iii
LIST OF TABLES	vi
LIST OF FIGURES	vii
LIST OF SYMBOLS	ix
LIST OF ABBREVIATIONS	xi
ABSTRAK	xii
ABSTRACT	xiv
CHAPTER 1 INTRODUCTION	1
1.1 General Introduction to Tsunami	1
1.2 Tsunami Formation	3
1.3 Tsunami Modeling	5
1.4 The Unpredictability of Tsunami	6
1.5 Objectives of Thesis	7
1.6 Methodology	8
1.7 Scope and Organization of Thesis	9
CHAPTER 2 LITERATURE REVIEW	11
2.1 Introduction	11
2.2 Numerical Models	12
2.3 Tsunami Generation	16
2.4 Tsunami Propagation	19
2.5 Tsunami Runup and Inundation	23

CHAPTER 3	TSUNAMI GENERATION	26
3.1	Introduction	26
3.2	Source Generation Terms	27
3.3	Okada Model	30
3.4	Experimental Studies and Explanation	32
3.5	26 December 2004 Andaman Tsunami	37
3.6	Conclusion	43
CHAPTER 4	MULTIGRID TSUNAMI SIMULATION MODEL TUNA	45
4.1	Introduction	45
4.2	In-house tsunami simulation model TUNA-M2	46
4.3	Numerical Experiments	49
4.3.1	Analytical vs. Nested TUNA-M1	50
4.3.2	Analytical vs. Nested TUNA-M2	53
4.3.3	Nested TUNA-M1 vs. Nested TUNA-M2	57
4.3.4	Nested vs. Non-Nested	59
4.3.5	TUNA-M2 vs. COMCOT	60
4.3.6	Friction vs. Non-friction	63
4.4	26 December 2004 Andaman Tsunami with Nesting in Langkawi	66
4.5	Conclusion	70
CHAPTER 5	TSUNAMI RUNUP AND INUNDATION	72
5.1	Introduction	72
5.2	In-house tsunami runup model TUNA-RP	74
5.3	Runup Height and Inundation Due to 26 December 2004 Andaman Tsunami	79
5.4	Conclusion	91

CHAPTER 6 CONCLUSIONS AND RECOMMENDATIONS 93

REFERENCES 96

LIST OF PUBLICATIONS 102

APPENDICES

Appendix A

Appendix B

LIST OF TABLES

	Page
3.1 Geological Terminology of a Shear Fault by Ben-Menahem and Singh (1981)	33
3.2 Parameters for Fault Model	39
3.3 Maximum wave height (m) and arrival time (h) at four observation points	43
3.4 Survey runup heights for the 26 December 2004 tsunami	43
4.1 Maximum wave height (m) and arrival time (h) at four observation points	70
5.1 Maximum wave height (m) at four observation points	73
5.2 Maximum runup heights at various seas bottom slope for Penang	85
5.3 Maximum runup heights at various seas bottom slope for Langkawi	90
5.4 Survey runup heights for the 26 December 2004 tsunami	91

LIST OF FIGURES

	Page
1.1 Map of Study Area (Wikimapia, 2008)	3
1.2 Tsunami wave generations by earthquake (Dias, 2008)	5
1.3 Tsunami wave generations by submarine landslides (ISDR, 2008)	5
2.1 Strike-slip faults (top) and dip-slip faults (bottom)	17
2.2 Faulting geometry and coordinate system by Mansinha and Smylie (1971)	18
3.1 Geometry of the earthquake source	29
3.2 Strike-slip faults (top) and dip-slip faults (bottom)	29
3.3 Geometry of the earthquake source model by Okada (1985)	31
3.4 Dip – slip fault and the correspond seismic wave for (a) Normal fault (b) Reverse fault (c) Detachment fault and (d) Thrust fault	35
3.5 Strike – slip fault and the correspond seismic wave for (a) Left lateral fault and (b) Right lateral fault	37
3.6 (a) Bathymetry and (b) computational domain with initial source	39
3.7 Snapshots of tsunami wave propagation towards peninsular Malaysia	40
3.8 Simulated wave heights at four observation points (a) Penang (b) Langkawi (c) Kantang and (d) Phuket	42
4.1 Computational grids for a staggered scheme	48
4.2 One dimensional multigrid computational domain	52
4.3 Analytical vs. TUNA-M1 for (a) elevation and (b) velocity with nested intervals	53
4.4 Two dimensional multigrid computational domain	55
4.5 Analytical vs. TUNA-M2 for (a) elevation and (b) velocity u and velocity v with nested intervals at several locations	56

4.6	Multigrid computational domains for (a) one-dimension and (b) two-dimension	57
4.7	TUNA-M1 vs. TUNA-M2 (Nested interval) at several locations	58
4.8	Nested vs. Non-Nested in TUNA-M2 at several locations	60
4.9	Snapshots of the tsunami waves at intervals of 500 s simulated by TUNA-M2 (top row) and COMCOT (bottom row) with applied nested grid	62
4.10	Elevation η (m) simulated by TUNA-M2 and COMCOT with applied nested grid at locations (4880, 14880) and (4920, 14920)	63
4.11	Friction vs. non-friction in TUNA-M2 for elevation at four locations	65
4.12	(a) Bathymetry and (b) computational domain with initial source	68
4.13	Contour plot of tsunami propagation towards Peninsular Malaysia and Thailand	68
4.14	Simulated wave heights at four observation points (a) Penang (b) Langkawi (c) Kantang and (d) Phuket	70
5.1	Staggered Schemes	75
5.2	A schematic sketch of the amount of water distributed to a particular dry cells	78
5.3	Study domain for Penang	81
5.4	Snapshots of the wave runup onto a bottom slope of 0.05 for Penang	82
5.5	Snapshots of the wave runup onto a bottom slope of 0.05 for Penang (enlarged dry land domain)	83
5.6	Study domain for Langkawi	86
5.7	Snapshots of the wave runup onto a bottom slope of 0.05 for Langkawi	87
5.8	Snapshots of the wave runup onto a bottom slope of 0.05 for Langkawi (enlarged dry land domain)	88
6.1	The local communities stay clear of the promenades along the beach in Penang	95

LIST OF SYMBOLS

<i>Symbols</i>	<i>Descriptions</i>	<i>Units</i>
c	wave celerity	ms^{-1}
g	acceleration due to gravitational force	ms^{-2}
h	water depth	m
d	water depth	m
H	offshore wave height	m
D	total depth	m
η	water elevation above the mean sea level (MSL)	m
w	water elevation above the mean sea level (MSL)	m
a	amplitude	m
t	time	s
T	wave period	s
M	discharge flux term in x- direction	m^2s^{-1}
N	discharge flux term in y- direction	m^2s^{-1}
n	manning Roughness coefficient	$\text{m}^{-1/3}\text{s}$
u	velocity of x component	ms^{-1}
v	velocity of y component	ms^{-1}
x	distance	m
y	distance	m
z	distance	m
ℓ	study domain size	m
Δx	grid size of x component	m
Δy	grid size of y component	m
Δt	time step	s
σ	wave frequency	s^{-1}
k	wave number	m^{-1}
σ_x	standard deviation of x component	m
σ_y	standard deviation of y component	m
R	maximum vertical runup height	m
α	bottom slope	m
β	bottom slope	m
v_k	outwards normal vector to surface	dimensionless

u_i^j	surface displacement	m
Σ	surface	m^2
S	surface	m^2
μ	Lamé constants for area	dimensionless
λ	Lamé constants for area	dimensionless
L	length of source area	m
W	width of source area	m
U	displacement of fault	m
ξ_i	source point	m
λ	slip angle	degree
δ	dip angle	degree
θ	strike angle	degree
N	latitude	degree
E	longitude	degree
F_{dry}	fraction of water allocated to each dry cell	dimensionless
ε	amplitude / depth	dimensionless
μ	depth / length	dimensionless
θ	Latitude	degree
φ	longitude	degree
R_e	Radius of the Earth	radian
f	Coriolis parameter	dimensionless
ω_e	Earth rotation frequency	radian

LIST OF ABBREVIATIONS

<i>Abbreviations</i>	<i>Descriptions</i>
LSWE	Linear shallow water equation
NSWE	Nonlinear shallow water equation
RANS	Reynolds-averaged Navier Stokes
VOF	Volume of fluid
MOC	Method of Characteristic

SIMULASI PENJANAAN, PERAMBATAN DAN ELEVASI MUKA AIR TERTINGGI DISEBABKAN TSUNAMI ANDAMAN 26 DISEMBER 2004

ABSTRAK

Tsunami Andaman 26 Disember 2004 telah membawa kesengsaraan kepada komuniti yang tinggal di kawasan persisiran pantai yang terjejas. Sejak itu, ahli sains dan komuniti tempatan berusaha sedaya upaya untuk menghasilkan langkah mitigasi tsunami. Pelbagai rancangan yang membina telah dibangunkan untuk tujuan ini, seperti pembinaan sistem amaran tsunami dan pembangunan model simulasi tsunami untuk menghasilkan peta evakuasi tsunami bagi kawasan yang terjejas. Fokus utama dalam tesis ini ialah pemodelan simulasi berangka bagi tiga fasa evolusi tsunami: penjanaan, perambatan dan elevasi muka air tertinggi. Untuk tujuan tersebut, satu siri model simulasi berangka tsunami bernama TUNA telah dibangunkan. TUNA memberikan kebolehan simulasi tsunami yang lengkap, bermula dengan pemodelan sumber tsunami yang disebabkan oleh gempa bumi dan berakhir dengan simulasi elevasi muka air tertinggi apabila menghampiri persisiran pantai. Satu model penjanaan yang bernama TUNA-GE dibangunkan mengikut konsep Okada dalam tesis ini. Model perambatan tsunami bernama TUNA-M2 yang dibangunkan dahulu, kini ditingkatkan kebolehan dalam keupayaan memilih grid terkandung untuk meningkatkan kejituan simulasi. Sumber tsunami yang disimulasi oleh model TUNA-GE digunakan untuk menghasilkan sumber permulaan bagi simulasi perambatan tsunami tersebut merentasi Laut India dengan menggunakan model perambatan tsunami TUNA-M2. Elevasi muka air tertinggi model TUNA-RP digunakan untuk simulasi elevasi muka air tertinggi dan elevasi muka air terendah untuk tsunami pada persisiran pantai yang cetek. TUNA-RP dibangunkan dengan berdasarkan persamaan air cetek tak linear dan keadaan pergerakan sempadan

digunakan untuk grid yang kecil. Model TUNA-RP digunakan untuk simulasi ketinggian elevasi muka air tertinggi untuk tsunami dan pembersihan pada persisiran pantai di Pulau Pinang dan Langkawi, dengan menggunakan ketinggian perambatan gelombang yang disimulasi oleh TUNA-M2 pada kadalaman laut 50 m sebagai input. Ketinggian elevasi muka air tertinggi di kawasan persisiran pantai Pulau Pinang dan Langkawi yang disimulasi mempunyai persetujuan yang baik dengan ketinggian elevasi muka air tertinggi yang diukur.

SIMULATION OF GENERATION, PROPAGATION AND RUNUP DUE TO THE 26 DECEMBER 2004 ANDAMAN TSUNAMI

ABSTRACT

The 26 December 2004 Andaman tsunami has resulted in much suffering among affected coastal communities. Since then, concerted effort among scientists and local communities has been devoted to provide tsunami mitigation measures. Several constructive programs have been developed for this purpose, such as the setting up of tsunami warning systems and the development of tsunami simulation models to produce tsunami evacuation maps for affected regions. The primary focus of this thesis is the numerical simulation of three distinct phases of tsunami evolution: generation, propagation and runup. For this purpose, a series of in-house numerical models TUNA has been developed. TUNA provides a complete suite of tsunami simulation capability, beginning with modeling the tsunami source generation resulting from an earthquake and ending with simulating runup along the coast. A generation model TUNA-GE is developed following the concept of Okada in this thesis. Previously developed tsunami propagation model TUNA-M2 is enhanced by the incorporation of nested grids to improve simulation resolutions. The tsunami source simulated by TUNA-GE model is used to provide the initial source to simulate tsunami propagation across the Indian Ocean by means of the enhanced propagation model TUNA-M2. The in-house runup model TUNA-RP is then used to simulate tsunami runup and rundown along shallow beaches. TUNA-RP was developed based upon the nonlinear shallow water equation with moving boundary condition using small grids. TUNA-RP model is used to simulate tsunami runup heights and inundation distances along the Penang and Langkawi beaches, using propagation wave height simulated by TUNA-M2 at 50 m depth as input. The

simulated runup height along Penang and Langkawi beaches are in good agreement with the survey runup heights.

CHAPTER 1

INTRODUCTION

1.1 General Introduction to Tsunami

The term tsunami was coined from the Japanese words consisting of harbor (tsu) and wave (nami). Tsunamis are also frequently referred as tidal waves, an exact translation from the ancient Greek name for a tsunami. But in actual fact, tsunami is not related to any tidal characteristic; hence, to avoid confusion with the tides, the term tidal wave is not used in scientific circles. Most tsunamis are triggered by underwater earthquakes (Satake, 2003); therefore, the term seismic sea waves are more appropriate in describing the tsunamis, although this term is seldom used.

A tsunami is a series of ocean waves formed when the sea floor is suddenly vertically shifted thereby creating an abrupt vertical displacement of huge volume of seawater. Earthquake, submarine landslide, volcanic eruption, meteorite impact, and human activities such as nuclear explosions in the ocean are some commonly known causes that may generate tsunami waves. Many tsunamis have occurred in the past ten decades; however, tsunamis are rare events as compared to other natural hazards such as earthquake and storm surge. Some of the largest historical tsunamis are the effect of earthquakes such as the Aleutian Earthquake and subsequent tsunami that occurred on 1st April, 1946 (Dudley and Lee, 1998), the Kamchatka Earthquake and Tsunami that occurred on 4 November, 1952 (USGS, 2008), the Aleutian Earthquake and Tsunami on 9 March, 1957 (Johnson et al., 1994). More recent tsunamis include the Chilean Earthquake and Tsunami on 22 May, 1960 (Dudley and Lee, 1998) and the Great Alaska Earthquake and Tsunami that occurred on 28 March, 1964 (USGS, 2008) and the most recent Andaman Earthquake and Tsunami that occurred on 26

December, 2004. Some of these tsunamis have caused casualties of hundreds of thousands people, injuries and tremendous damages to infrastructures and properties. The Andaman tsunami, which occurred on 26 December 2004, is one of the most devastating tsunami in the history of mankind. This tsunami was triggered by a mega-earthquake with the Richter scale of 9.3, off the west coast of northern Sumatra near the Province of Aceh and resulted in fatalities of about 250, 000 in more than ten countries. This tsunami has awakened countries around the Andaman Sea regarding the hazards of tsunamis and the needs of mitigation actions. Since then, numerous researches on tsunami such as the development of tsunami simulation models have been undertaken in order to mitigate the adverse impacts of tsunamis in the near future. Coupled with these researches, there are numerous other efforts put up by concerned community and governments such as the setting up of early warning systems, community education, disaster evacuation planning and preparedness to face the potential impacts from this Mother Nature's disaster.

There are scientific indications that tsunamis are very likely to recur and pose great risks and hazards to those countries encircling the Andaman Sea, as there are high possibilities that earthquakes will occur again in this region. Since the region is sensitive and theoretically vulnerable to tsunami's strikes, it is essential to construct a comprehensive tsunami mitigation plan based on possible risks that a tsunami may pose. Hence, the aim of this thesis is to formulate a credible and realistic modeling of the 26 December 2004 Andaman tsunami for the location of peninsular Malaysia. In Figure 1.1, the rectangle is the map of the study area. This thesis also discusses about the nature and basic characteristics of a tsunami and the potential risks it poses to those affected areas.



Figure 1.1 Map of Study Area (Wikimapia, 2008)

1.2 Tsunami Formation

The most common tsunamigenic events are underwater earthquakes that could produce a co-seismic deformation that causes displacement of a huge body of water, as shown in Figure 1.2 (Dias, 2008). This seabed deformation is normally caused by a subduction when two oceanic plates slip through each other at the contact region known as the plate boundary. The energy of that fault is transferred to the water and elevates the water upward exceeding the normal sea level (Koh et al., 2007). The length scale of this sea floor deformation is much larger than the water depth, which forms the initialization of the tsunami wave generation called the initial-conditions. It is presumed that the initial sea surface deformation is equal to the co-seismic vertical displacement of the sea floor. This is the birth of the seismic waves. Tsunamis may also be triggered by a violent horizontal displacement of water such as submarine landslide in the ocean as shown in Figure 1.3 (ISDR, 2008). For tsunami generated by submarine landslides, the initial waveforms at the source are more difficult to derive. The wavelengths are shorter, implying the increased significance of wave dispersion in subsequent propagation.

Subsequent to the vertical uplift, the displaced water column then splits into two opposing directions. The transoceanic tsunamis waves can travel at high speeds exceeding 100 m/s, with long period and long wave-length in a deep ocean. This stage is known as tsunami propagation as shown in Figure 1.2(c) and 1.3(c). The travelling speed depends on its wavelength, water depth, friction and slope. As the wave's propagation reaches the shallow coastal areas, the wavelengths are reduced thus slowing down the wave but are amplified in heights and velocities to reach the maximum vertical heights onshore, creating a destructive situation that can pose great danger to humans and properties. This final stage of a tsunami's evolution creates a dissemination of the waves with different frequencies or spectra and with different propagation speeds. This is known as tsunami runup and inundation.

Tsunamis generated by the sudden vertical elevation of water column such as those caused by earthquakes are far better understood than those caused by submarine landslides (Teh, 2008). Submarine landslides are oftentimes the aftermath events that accompany major earthquakes, which are very likely to add up the overall power of a tsunami or creating additional tsunami waves. The most dangerous and devastating tsunami is a tsunami generated by submarine landslides located nearby to the coastal areas with distance less than several hundreds km and is known as near-field tsunami. These types of tsunamis are considered more dangerous than those created in deep ocean uplift of similar volume because the potential energy of these tsunamis could be much higher and more focused. Reason for this to happen is because the slide depth could be in the order of thousands of meters, as compared with uplift, which is capped by the vertical displacement of the seafloor, which rarely exceeds 10 m. Hence, near field tsunami triggered by submarine landslides can be devastating.

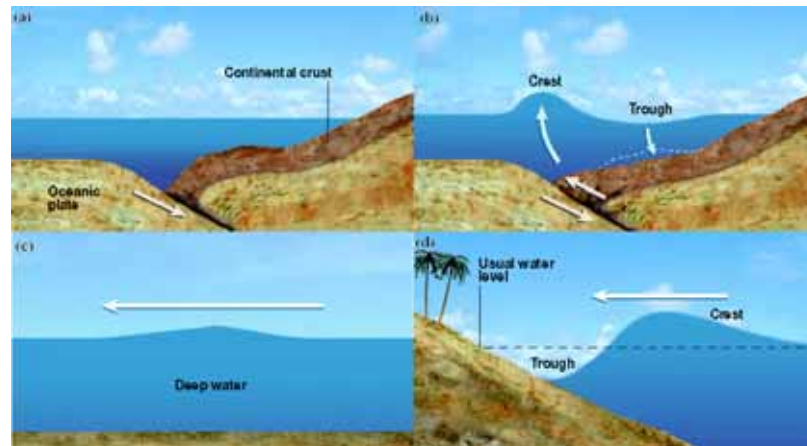


Figure 1.2 Tsunami wave generations by earthquake (Dias, 2008)

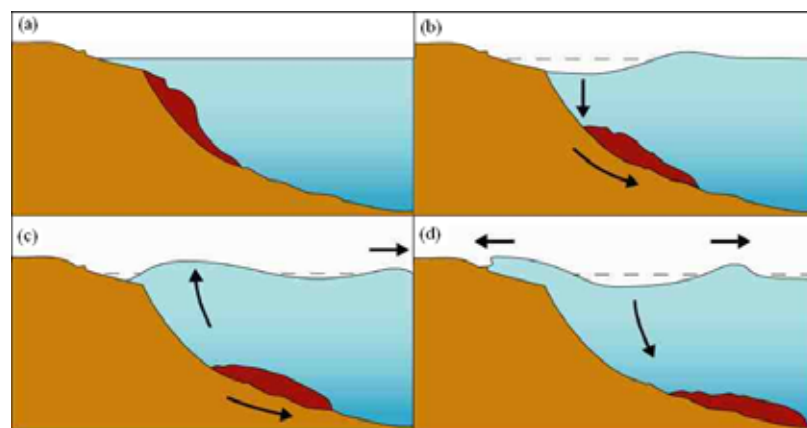


Figure 1.3 Tsunami wave generations by submarine landslides (ISDR, 2008)

1.3 Tsunami Modeling

After the devastating 2004 Andaman tsunami, tsunamis have become a major topic of concern among researchers, geologists and oceanographers. There are scientific indications that tsunami of similar magnitude may recur in this region due to the energy that has yet to be released. In fact, earthquakes of lesser scale have triggered several tsunamis after the 2004 Andaman tsunami. This includes the Java earthquake at the southern Java, Indonesia with the magnitude of 7.7 on 17 July 2006 and the Solomon earthquake of magnitude 8.1 on 2 April 2007 in Solomon Islands. Hence, sensitivity to the needs for preparedness and mitigation to face potential hazards posed by future tsunamis has been a driving force for developing tsunami

resilience communities. Various efforts on community disaster management and risk mitigation capabilities are undertaken by government and concerned communities in order to help mitigate the potential impacts and risks on coastal communities. Numerical simulations of tsunami risks are one of the integral components of the capacity building for community disaster management. These numerical simulations are crucial in developing inundation and evacuation maps for the purpose of providing effective mitigation measures and to help developing risk management strategies. Moreover, numerical simulations can provide scientifically sound tsunami data such as wave amplitude, arrival times as well as current velocities of tsunamis, which are vital in spearheading the process of protecting, rescuing and recovering operations before and after the strikes. In this regards, tsunami modeling is a topic that is worthy to be researched in details because of its pragmatic considerations.

1.4 The Unpredictability of Tsunami

Indeed, there are scientific ways to identify the fault areas that could cause earthquakes that are very likely to accumulate enough energy to lead to more quakes in future. But predicting when exactly it will happen is not easy. The missing part to pinpoint the next quakes or tsunamis is not the mathematical formulas, but the real data, which lies too far out of reach, miles deep in the earth. Therefore, it is hoped that tsunami modeling could help in the mitigation process in reducing the devastating impact since preventing it is impossible.

Since it is difficult to predict when a tsunami will occur, much effort are turned to warning system which ideally could notify coastal communities for evacuation before the arrival of the devastating waves. However, it should be noted that early warning system are designed to be sensitive as it cannot afford to miss any real encounter, therefore triggering a false alarm is a norm, with the Pacific Ocean

early warning system's false alarm rate been estimated at 75 percent. One of the examples was the Bengkulu earthquake, which occurred on 12 September 2007. The earthquake with the magnitude of 8.4 Richter scale and the aftershock of magnitude 6.6 Richter scale generated a tsunami alert that was subsequently called off. This happened mainly due to different variations in coastal amplification factors and because seismic data often translate to tsunami data imprecisely. False alarms are not only costly in term of money; a statewide evacuation of Hawaii was estimated at USD 68 million (Teh, 2008). But false alarms that recur too frequently may desensitize response to future real alarms, causing people to ignore these real alarms, thus rendering the early warning system ineffective to protect communities affected. In this regards, it is hoped that early warning system can be enhanced by using tsunami modeling in order to reduce errors and costs. For this purpose TUNA was developed by a team of modelers in the Universiti Sains Malaysia (USM) to provide a complete package of capability to simulate the entire process of tsunami generation at the source of earthquake, propagation in the deep ocean and final runup along shallow beaches. We envisage that in the near future we will incorporate other physical and ecological process sub models into TUNA so that it has the additional capability to simulate sediment transport associated with tsunami, as well as to simulate environmental and ecological processes such as storm surge and water quality.

1.5 Objectives of Thesis

The objectives of this thesis are as follows:

1. To develop tsunami generation model TUNA-GE;
2. To implement tsunami generation model TUNA-GE for the purpose of generate credible source trigger by earthquake;

3. To enhance tsunami propagation models TUNA-M2 by utilizing nested grid for improving simulation resolutions;
4. To implement an enhanced tsunami propagation model TUNA-M2 for the purpose of simulate tsunami wave heights offshore the Langkawi and Penang coast;
5. To implement tsunami runup model TUNA-RP for the purpose of simulate tsunami runup heights and inundation distances along the Penang and Langkawi beaches.

1.6 Methodology

1. Generation model is developed based on principles in earlier theoretical studies in the literature.
2. Finite difference technique is used to solve linear and nonlinear shallow water equations, based on staggered scheme and developed computer simulations to simulate tsunami propagation and runup.
3. Enhancement of propagation model based on linearly interpolation technique for the boundaries and finite difference technique for the inner grids.
4. A soliton is prescribed as a single hump of the Gaussian in the runup model as the initial condition. Moving boundary condition is imposed in the runup model to resolve the shoreline movement problem and allow the tsunami wave to propagate over a dry bed region. Radiation boundary condition is imposed in the runup model to allow the waves to pass through the open boundary freely without reflection.
5. Computational results of a generated ideal situation are compared with known analytical solutions. Comparison is made also with other model (COMCOT) and in order to validate the accuracy of enhanced TUNA model.

6. Simulated results with real case's parameters from literature are compared with survey data for the 2004 Andaman tsunami.

1.7 Scope and Organization of Thesis

This thesis has been designed to consist of six chapters. In Chapter 1, a general introduction to tsunami is given. The overall theme of this research is then discussed in this chapter. The objectives, scope and organization of this thesis are presented at the end of this chapter.

Chapter 2 presents literature review of the tsunami wave generation, propagation and runup. Some existing numerical models are briefly discussed in this chapter. Moreover, some other method for describing multi-grid coupled model is presented in this chapter.

Chapter 3 begins with a brief introduction to the 26 December 2004 Andaman tsunami and to study tsunami generation. Some review of source generation term produced by an earthquake is briefly presented here. Combination of a variety of source generation is considered in order to generate a credible source for the 2004 Andaman tsunami. In this chapter, a generation model following the concept of Okada is incorporated into an in-house tsunami generation model named TUNA-GE. Before the TUNA-GE model is developed, a review of the Okada concept is described. Some experimental studies and explanation of the surface deformation are briefly explored in this chapter. This chapter ends by simulating tsunami propagation for the 2004 Andaman tsunami by using the credible source generated by TUNA-GE model.

We continue with Chapter 4 by enhancing the in-house propagation model TUNA-M2 by incorporating nested grid in order to improve the simulation resolutions. This chapter begins with the introduction to the shallow water equations

that are employed in TUNA-M2 model and the finite difference method that is used to solve the shallow water equations. This chapter continues with some validation of the enhanced TUNA-M2 model by several methods such as analytical model in one and two dimensions and by comparison with other existing models like COMCOT. This chapter ends by simulating the 2004 Andaman tsunami with the initial condition obtained from TUNA-GE model.

In Chapter 5 a well-tested in-house runup model TUNA-RP is used to simulate the runup heights and inundation distances along the beaches in Penang and Langkawi. This chapter begins with an introduction to nonlinear shallow water equations and the explicit finite difference method used in TUNA-RP model. Two boundary conditions are imposed in TUNA-RP model, which are open radiation boundary condition and moving boundary condition, which will be described in this chapter. Runup heights and inundation distance along the beaches of Penang and Langkawi are obtained at the end of this chapter, using as input the offshore wave heights obtained earlier in Chapter 4. The simulated tsunami runup heights and inundation distances along the Penang and Langkawi beaches are then compared with the surveyed runup heights and inundation distances observed by a survey team from USM conducted.

Chapter 6 discusses the overall conclusions of this thesis. Some expositions and recommendations for further research on enhancing tsunami modeling are also provided in this final chapter.

CHAPTER 2

LITERATURE REVIEW

2.1 Introduction

The Sumatra-Andaman earthquake on the Richter scale of 9.3 occurred on 26 December 2004, off the west coast of northern Sumatra near the Province of Aceh. This earthquake triggered off a series of large tsunamis that caused tremendous damage to properties and resulted in fatalities of around 250, 000 along the affected coastal regions. Although Malaysia was previously perceived as safe from tsunami hazards, Penang, Langkawi and parts of northwest Malaysia were not spared the agony caused by the tsunami. A total of 68 persons were killed in Malaysia, with 32 death in Penang alone (Koh et al., 2007). There are scientific indications that significant tsunamis may occur again and pose great risks and hazards to this region in the near future. Precise assessment of tsunami impacts and risks is crucial in identifying mitigation measures that could be carried out in order to reduce the threat of tsunami toward coastal communities. However, essential information such as the likelihood of occurrence, magnitude, shape of the sea bed deformation, topography and location of tsunamigenic events are rarely available before any tsunami strikes, thus complicating the process of risk maps creation. However, as more information becomes available in the future, tsunami assessments using computer models should increase in accuracy.

Presently, several numerical models have been developed to simulate specifically a few or entire phases of a tsunami evolution. These numerical models can be used to determine the tsunami wave heights, the travel time and the potential impact that a tsunami could cause. These numerical models include COMCOT

(COrnell Multigrid COupled Tsunami) model (Liu et al., 1998; COMCOT, 2007), MOST (Methods of Splitting Tsunami) model developed by Titov and Synolakis (1998), TUNAMI-N2 models developed by Imamura of Tohoku University (Imamura et al., 1988) and TUNA model developed by Koh et al. (2005). Although Malaysia was previously perceived as safe from tsunami threat, the 2004 Andaman tsunami has caused agony to the communities of Malaysia. Consequently, tsunami simulation model became an urgent necessity in mitigating tsunami impact. However, due to proprietary ownership of other simulation models, TUNA model was developed as an in-house simulation tool to prevent copyright issues. Further discussions regarding these numerical models will be briefly touched on in next section.

2.2 Numerical Models

Tsunami numerical models are mainly designed with the objective of simulating a past event to further understand the behavior of tsunami, to analyze or to predict future impacts on potentially vulnerable areas. Several numerical models have been developed worldwide by universities and research centers. Numerical models are also widely used in tsunami forecasting systems.

COMCOT

The numerical model COMCOT was created by Liu et al. (1998) of Cornell University. This model is used for simulating tsunami generation, propagation and runup. The initial source generation for earthquake, submarine landslide, wave maker and initial surface file are developed and can be used in this model. Linear shallow water equations are used to simulate distant propagation of tsunamis while nonlinear shallow water equations are used to simulate tsunami runup and inundation. In this

model, different coordinate systems such as Cartesian coordinate system or Spherical coordinate system can be utilized. Linear or nonlinear shallow water equations are discretized by using explicit leap-frog finite difference scheme, the convective term in the nonlinear shallow water equations are discretized by using an upwind scheme. This model has incorporated a nested multi-grid system and can be applied in specific sub region for the purpose of accuracy, the details of which will be discussed later. A moving boundary treatment is applied to track movement of the shoreline. The COMCOT model has been used to simulate the 1960 Chilean tsunami (Liu et al., 1994), the 1986 Hwa-Lien Taiwan tsunami (Wang and Liu, 2005), the 2004 Andaman tsunami (Wang and Liu, 2006; 2007) and also the Ping-Tung Taiwan submarine earthquake that occurred on December 26, 2006 (Chen, 2007), even though this earthquake did not cause any tsunami hazards, but the tidal gages had recorded long water waves near the epicenter.

MOST

The method of splitting tsunami model (MOST) was developed by Titov and Synolakis (1998). This model was developed also based upon the shallow water equations. This model is able to compute all three phases of tsunami evolution, which are tsunami generation, propagation, and runup, thus providing a complete tsunami simulation capability. The Pacific Disaster Center in Hawaii utilizes MOST model to develop tsunami hazard mitigation tools. This model is associated with the activities of the Tsunami Inundation Mapping Efforts (TIME). MOST does not include bottom friction term in its formulation as it is not an important factor in deep oceans and it is very difficult to determine the friction coefficients a priori.

TUNAMI-N2

TUNAMI-N2 is another well-known tsunami model, developed by Imamura of Tohoku University (Imamura et al., 1988). It is provided through the Tsunami Inundation Modeling Exchange (TIME) program (Goto et al., 1997). This model includes friction term, which is omitted in MOST and is optional in TUNA models. TUNAMI-N2 model is used for studying tsunami propagation and runup. Several real case studies have used TUNAMI-N2 to model tsunami wave field such as the Mediterranean (Pelinovsky et al., 2002), the Carribean Sea (Zahibo et al., 2003), the Black Seas (Yalciner et al., 2004) and the Java Sea (Zahibo et al., 2006).

COULWAVE

The name of the model, COULWAVE (Lynett and Liu, 2004) came from Cornell University Long and Intermediate Wave Modeling Package. Lynett et al. (2002) used depth-integrated model for waves in intermediate water and linear interpolation for waves near the wet-dry boundary. This model was developed based upon the Boussinesq-type equations for weakly dispersive waves. The Boussinesq-type of equations used is shown as follows:

$$\frac{\partial \eta}{\partial t} + \frac{\partial M}{\partial x} + \frac{\partial N}{\partial y} = 0 \quad (2.1)$$

$$\frac{\partial M}{\partial t} + \varepsilon \left[\frac{\partial}{\partial x} \left(\frac{M^2}{H} \right) + \frac{\partial}{\partial y} \left(\frac{MN}{H} \right) \right] + H \frac{\partial \eta}{\partial x} = \mu^2 \frac{h^3}{3} \left[\frac{\partial^3 \eta}{\partial x^3} + \frac{\partial^3 \eta}{\partial x \partial y^2} \right] + O(\mu^4, \varepsilon \mu^2) \quad (2.2)$$

$$\frac{\partial N}{\partial t} + \varepsilon \left[\frac{\partial}{\partial x} \left(\frac{MN}{H} \right) + \frac{\partial}{\partial y} \left(\frac{N^2}{H} \right) \right] + H \frac{\partial \eta}{\partial y} = \mu^2 \frac{h^3}{3} \left[\frac{\partial^3 \eta}{\partial x^2 \partial y} + \frac{\partial^3 \eta}{\partial y^3} \right] + O(\mu^4, \varepsilon \mu^2) \quad (2.3)$$

where

η – water elevation above the mean sea level, m;

h – water depth, m;

H – total water depth, m;

M – discharge flux term in the x- direction, m^2s^{-1} ;

N – discharge flux term in the y- direction, m^2s^{-1} ;

ε – amplitude / depth;

μ – depth / length;

The right side of the Equations (2.2) and (2.3) are frequency dispersion while the left side of the Equations (2.2) and (2.3) are shallow water equations. The Boussinesq-type equation with frequency dispersion caused the model computation to be extremely slow and may not be suitable to simulate transoceanic wave (Horrillo and Kowalik, 2006; Liu et al., 2008). Hence, Boussinesq-type of equation is beyond the scope of this thesis. However, this model has been applied to one-dimensional and two-dimensional cases where the moving boundary technique achieves numerical-stability. The comparison results indicate a significant improvement over weakly nonlinear Boussinesq equation results of Zelt (1991).

TUNA

TUNA model developed by Teh et al. (2005; 2006) is a tsunami simulation model, consisting of two components namely TUNA-M2 and TUNA-RP. TUNA-M2 model is a tsunami propagation model developed by Teh et al. (2005) following the guidelines of UNESCO/IOC working group (IOC, 1997) to simulate tsunami wave height off the coast at a depth of about 30 m. The model uses elliptical hump $\eta = ae^{-(x/\sigma_x)^2} \times e^{-(y/\sigma_y)^2}$, where a is the wave amplitude, σ_x and σ_y are the standard deviations in x- and y- directions respectively, to fit the initial wave (Yoon, 2002), as the source generation or initial water surface disturbance. The shallow water equations are used to describe the subsequent tsunami propagation in the deep ocean, since tsunami wavelengths (of hundreds of km) are typically much larger than the ocean depths (kms), which in turn are much larger than the wave heights (m),

tsunamis are categorized as shallow water wave (SWW). In TUNA-M2 model, an explicit finite difference method is used to solve a set of partial differential equations that describe shallow water equations. The model has been used to simulate the 2004 Andaman tsunami with a source near the Province of Aceh, propagation towards peninsular Malaysia (Teh et al., 2005; Koh et al., 2008a) and propagation towards Bay of Bengal by Cham (2007). TUNA-RP model is also an in-house model that is used to simulate tsunami runup heights and inundation distances by using the input wave height off shore at 50 m depth derived from the TUNA-M2 model. This TUNA-RP model is executed by using one-dimensional nonlinear shallow water equations, which is also solved by using explicit finite difference method. A moving boundary condition is used in this model to simulate tsunami runup height and inundation distance along the beaches. This model has been used to simulate tsunami runup and inundation along the Penang beaches by Teh et al. (2006; 2008).

2.3 Tsunami Generation

In this section, we will review some methods to represent tsunami generation caused by an earthquake. When an earthquake occurs near the seabed, caused by a sudden slip of a fault, it triggers a perturbation of the sea floor that produces a co-seismic deformation. The sea floor disturbance will reshape the sea surfaces into tsunami waves where the initial sea surface displacement will lead to tsunami being generated. Due to the incompressibility of sea water, this sea surface displacement is assumed to be equivalent to the seabed displacement. According to Mansinha and Smylie (1971), co-seismic deformation is usually caused by strike-slip fault and dip-slip fault.

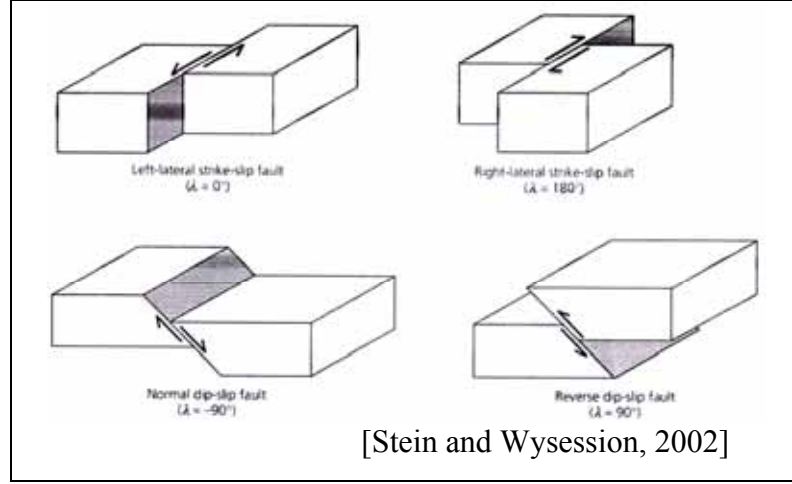


Figure 2.1 Strike-slip faults (top) and dip-slip faults (bottom)

A closed form analytical expression for the displacement field for strike-slip fault and dip-slip fault was given by Mansinha and Smylie (1971). The model is known as elastic half-space dislocation model. The elastic dislocation model is developed based upon the theory of elastic dislocation, which uses dislocation to determine the displacement field in a uniform half-elastic, and is given as below:

$$u_i = \int_{\Sigma} \Delta u_j \left[\lambda \delta_{jk} \frac{\partial u_i^l}{\partial \xi_l} + \mu \left(\frac{\partial u_i^j}{\partial \xi_k} + \frac{\partial u_i^k}{\partial \xi_j} \right) \right] v_k dS_i \quad (2.4)$$

where Δu_j is the elementary dislocation, δ_{jk} is the dip angle, dS_i is the dislocation surface, v_k denotes outwards normal vector to surface Σ , λ and μ are the Lamé constants for area, u_i^j is a i th component facing a point force of unit magnitude at (ξ_1, ξ_2, ξ_3) acting in the j -direction that causes the displacement at (x_1, x_2, x_3) . There are other fault models such as Okada model (Okada, 1985) which will be discussed in later chapter.

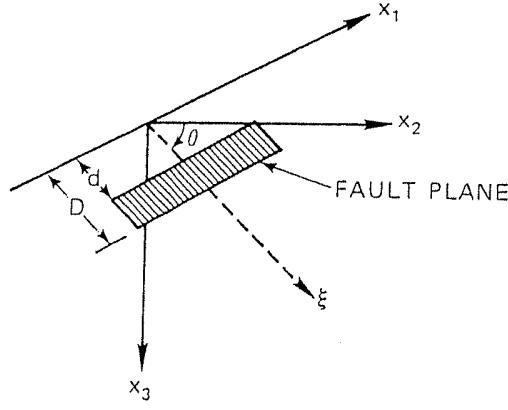


Figure 2.2 Faulting geometry and coordinate system by Mansinha and Smylie (1971)

The geometry of the finite rectangular faulting source model and the coordinate system used in Mansinha and Smylie (1971) are shown in Figure 2.2. In this coordinate system, the analytical expressions for the displacement field of the strike-slip fault and dip-slip fault caused by a uniform slip are given as follows:

Strike-slip fault

$$u_i = \mu U_1 \int_d^D \int_{-L}^L \left[\left(\frac{\partial u_i^1}{\partial \xi_2} + \frac{\partial u_i^2}{\partial \xi_1} \right) \sin \delta - \left(\frac{\partial u_i^1}{\partial \xi_3} + \frac{\partial u_i^3}{\partial \xi_1} \right) \cos \delta \right] d\xi_1 d\xi_2 \quad (2.5)$$

Dip-slip fault

$$u_i = \mu U \int_d^D \int_{-L}^L \left[2 \left(\sin \delta \frac{\partial u_i^2}{\partial \xi} - \cos \delta \frac{\partial u_i^3}{\partial \xi} \right) + \left(\frac{\partial u_i^3}{\partial \xi_2} - \frac{\partial u_i^2}{\partial \xi_3} \right) \right] d\xi_1 d\xi_2 \quad (2.6)$$

in which the elementary dislocations U_1 and U correspond to strike-slip and dip-slip respectively. The symbol δ denotes dip angle and the finite rectangular fault surface is assumed to cover the range of $-L \leq \xi_1 \leq L$ and $d \leq \xi_2 \leq D$ as in Figure 2.2. The integrals of the strike-slip and dip-slip displacements can be obtained in Mansinha and Smylie (1971).

2.4 Tsunami Propagation

Tsunami propagation is the second phase of tsunami evolution. In this stage, the wave propagation begins from the source generated by an earthquake towards the offshore of the coast, with the tsunami as the medium to transfer the seismic energy away from the source. Tsunami is considered a shallow water wave since the wavelengths are much larger than the ocean depths; hence, linear shallow water equations are used in numerical simulation to express tsunami propagation. The shallow water equations that describe the conservation of mass and momentum can be depth averaged (Hérbert et al., 2005) and are usually represented in Cartesian coordinate form as Equations (2.7) to (2.9) (Ippen, 1966; IOC, 1997) or in Spherical coordinate form as Equations (2.10) to (2.12) (Nagano et al., 1991; Titov et al., 2005).

$$\frac{\partial \eta}{\partial t} + \frac{\partial M}{\partial x} + \frac{\partial N}{\partial y} = 0 \quad (2.7)$$

$$\frac{\partial M}{\partial t} + \frac{\partial}{\partial x} \left(\frac{M^2}{D} \right) + \frac{\partial}{\partial y} \left(\frac{MN}{D} \right) + gD \frac{\partial \eta}{\partial x} + \frac{gn^2}{D^{7/3}} M \sqrt{M^2 + N^2} = 0 \quad (2.8)$$

$$\frac{\partial N}{\partial t} + \frac{\partial}{\partial x} \left(\frac{MN}{D} \right) + \frac{\partial}{\partial y} \left(\frac{N^2}{D} \right) + gD \frac{\partial \eta}{\partial y} + \frac{gn^2}{D^{7/3}} N \sqrt{M^2 + N^2} = 0 \quad (2.9)$$

where

η = Water elevation above mean sea level (MSL), m;

h = Water depth, m;

g = Gravitational acceleration, ms^{-2} ;

n = Manning Roughness coefficient, $\text{m}^{-1/3}\text{s}$;

$D = h + \eta$ = Total water depth, m;

$M = uD$ = Discharge flux in the x- direction, m^2s^{-1} ;

$N = vD$ = Discharge flux in the y- direction, m^2s^{-1} ;

u = Velocity of x- direction, ms^{-1} ;

v = Velocity of y- direction, m^2s^{-1} .

$$\frac{\partial \eta}{\partial t} + \frac{1}{R_e \cos \theta} \left[\frac{\partial M}{\partial \varphi} + \frac{\partial}{\partial \theta} (N \cos \theta) \right] = 0 \quad (2.10)$$

$$\frac{\partial M}{\partial t} + \frac{gh}{R_e \cos \theta} \frac{\partial \eta}{\partial \varphi} = fN \quad (2.11)$$

$$\frac{\partial N}{\partial t} + \frac{gh}{R_e} \frac{\partial \eta}{\partial \theta} = -fM \quad (2.12)$$

where

θ = Latitude;

φ = longitude;

R_e = Radius of the Earth;

$f = 2\omega_e \sin \theta$ = Coriolis parameter;

ω_e = Earth rotation frequency;

M = Discharge flux along the latitude;

N = Discharge flux along the longitude;

$h(x,y)$ = unperturbed water depth.

COMCOT (Liu et al., 1998; COMCOT, 2007) is one of the numerical simulations that uses both coordinate systems. Spherical coordinate system is used when a curvature of the earth is considered important for waves propagate over a long distant from approximately 1000 km up to 10000 km. There are a lot of existing numerical simulations available to simulate tsunami propagation.

In the natural environment, bathymetry varies from one location to another. In other words, it will not be constant. In the case when the water depth is shallow, a smaller grid size for numerical simulation is required in order to obtain a better resolution. Hence, a refinement of the numerical mesh used in simulations may be needed for these purposes. The COMCOT model (Liu et al., 1998; COMCOT, 2007) is capable of making refinement by incorporating nested multi-grid system, which

can be applied in specific region, especially for the shallow depth. Next we will discuss the Multi-grid coupled model applied in the COMCOT model.

Multi-grid Coupled Model

As we have mentioned before, COMCOT incorporates a nested multi-grid system that can be applied in specific subregion. The options of linear or nonlinear shallow water equations with different subcoordinate system such as Cartesian or Spherical can also be chosen and applied to each specific subregion. In between two adjacent subregions, any ratio of grid sizes are flexible to be used and all these subregions are dynamically connected. Below is the algorithm describing the technique for exchanging information in between two subregions of different grid sizes. In this case, a small grid system is nested in a large grid system with the ratio of grid size set to be equal to 1:3. Suppose all flux values in the outer region are known at time level $t = t_1$. The values at the next time step $t = t_2$ are to be determined for the inner and the outer regions. The time step used in a smaller grid system is smaller than the time step used in larger time step system, to satisfy the Courant-Friedrichs-Lewy stability condition, $c \times dt / dx < 1$ (Liu et al., 1998).

The algorithm for exchanging information between two subregions of different grid sizes is given below:

1. After the flux values for the outer region at t_1 are obtained, the free surface elevation at $t_{1+1/2}$ in the outer region can be solved by using continuity equation (conservative of mass).
2. The flux values in the inner region at time level $t = t_1$ are obtained by solving the momentum equation. But the flux values along the connected boundary at this time level must be obtained by linearly interpolating the flux values in the outer region at the same time level, which is $t = t_1$. The

- interpolated values obtained are then assigned to the boundary for inner region.
3. The flux values in the inner region at t_1 are used to solve the free surface elevation at $t_{1+1/4}$ in the inner region by solving continuity equation.
 4. After the free surface elevation at $t_{1+1/4}$ is obtained, the flux values at the next time step $t_{1+1/2}$ (for small region) is solved by using the momentum equation. The flux values along the connected boundary for this time level may not be obtained in this step. The next step will describe how to get the flux values along the connected boundary.
 5. By using the flux values at t_1 and free surface elevation at $t_{1+1/2}$, the flux values along the connected boundary at t_2 for the outer region can be obtained locally by solving the momentum equation. Next, the flux values along the connected boundary in the outer region at time level $t = t_2$ are then linearly interpolated and the interpolated values obtained are then assigned to the boundary for inner region at t_2 . Time averaging is used for the flux values in the outer region at t_1 and t_2 and the time averaged values are then assigned to obtain the flux values in the inner grid at the boundary $t_{1+1/2}$.
 6. The free surface elevation at $t_{1+3/4}$ in the inner region can be obtained by solving the continuity equation with the flux values for inner region obtained in Step 4 and 5.
 7. Up to this step, the flux values for the inner region at t_1 , $t_{1+1/2}$ and free surface elevation for the inner region at $t_{1+1/4}$, $t_{1+3/4}$ is obtained. The values are needed to transfer back from the inner region to the outer region to update the outer region. Hence, the free surface elevation in the inner

region is spatially averaged over the grid size of the outer region. Next, time averaging is used again for the averaged elevation at $t_{1+3/4}$ with the free surface elevation at $t_{1+1/4}$ in the inner region. These spatially and time averaged elevation values in the inner region are then used to update the free surface elevation values at $t_{1+1/2}$ in the outer region.

8. The flux values at t_2 in the inner region can be obtained by solving the momentum equation.
9. The flux values at t_2 in the outer region can be also obtained by solving the momentum equation.

2.5 Tsunami Runup and Inundation

As the tsunami wave propagates up to shallow beaches, the linear shallow water equations (LSWE) that is normally used for the tsunami propagation over the deep ocean is no longer valid. In this phase, a nonlinear shallow water equations (NSWE) with its convective inertia force and bottom friction with the seabed needs to be considered. Many researches recently have concluded that the neglect of nonlinearity for runup simulation will tend to underestimation of the predicted maximum wave height. NSWE including bottom frictional effects is sufficient in describing the flow motion of the coastal zone (Liu et al., 1994). A simple NSWE (Marchuk and Anisimov, 2001; Gedik et al., 2005; Marchuk) is as follows:

$$\frac{\partial \eta}{\partial t} + \frac{\partial(u(\eta + h))}{\partial x} = 0 \quad (2.13)$$

$$\frac{\partial u}{\partial t} + u \frac{\partial u}{\partial x} + g \frac{\partial \eta}{\partial x} = 0 \quad (2.14)$$

where

η = surface elevation, m;

u = velocity, m/s;

h = water depth, m;

g = gravitational acceleration, m/s^2 ;

t = time, s;

x = distance, m.

There are also numerical models developed based on other equations such as the Boussinesq equations and the Reynolds-averaged Navier-Stokes (RANS) equations. Petit et al. (1995) developed the model SKYLLA based on RANS and FLAIR method for simulation of runup on coastal structure. A numerical technique based on volume of fluid (VOF) for simulating the high wave of distorted water-air interfaces was proposed in Sabeur et al. (1997). Kawasaki (1999) proposed a two-dimensional numerical wave model that combines the VOF method with a non-reflective wave generator. Lin and Liu (1998) have proposed a RANS based numerical model with k - ϵ equations to study the evolution of wave train, shoaling and breaking in the surf zone. Xiao et al. (2007) proposed a numerical model based on RANS and k - ϵ equations to simulate solitary wave runup and forces acting on an idealized beachfront house on a plane beach.

In numerical models, moving boundary technique is often used to investigate wave runup and rundown with depth integrated equations such as in Lynett et al. (2002). Some researchers added bottom friction and eddy viscosity into momentum equations in order to reduce the computational instabilities.

Other than numerical solutions, there are also theoretical formulations that describe the maximum runup of solitary wave on impermeable plane slope. Nonlinear shallow water equations may be approximated by analytical approaches to study the maximum runup of solitary wave, disregarding dispersion and other higher order effects for simplicity (Yeh et al., 1996; Xiao et al., 2007). Synolakis (1986;